



Cite this: *Dalton Trans.*, 2016, **45**, 15886

Received 31st May 2016,
Accepted 15th June 2016
DOI: 10.1039/c6dt02185a

www.rsc.org/dalton

Ligand effects on the properties of Ni(III) complexes: aerobically-induced aromatic cyanation at room temperature†

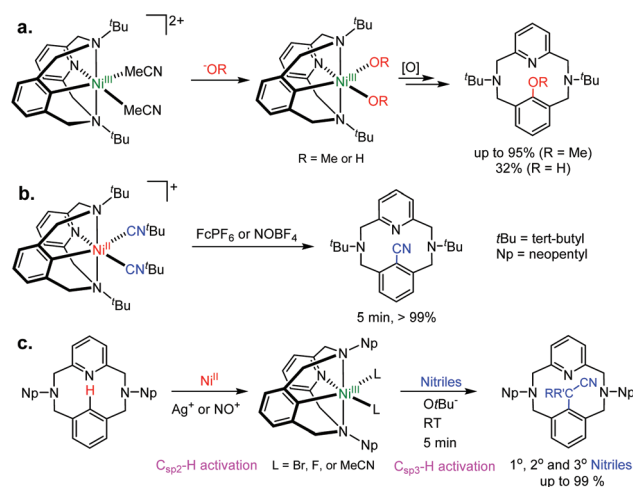
Wen Zhou,^a Michael B. Watson,^a Shuai Zheng,^a Nigam P. Rath^b and Liviu M. Mirica*^a

A series of organometallic Ni^{II} and Ni^{III} complexes supported by tetradentate ^RN₃C⁻ ligands were synthesized and fully characterized using X-ray crystallography, CV, and EPR. Based on the solid state structures, the substituents on the two amine N-donors significantly affect the coordination of the Ni^{III} centers, while the *para* substituents of the phenyl C-donor have a reduced effect. This is further supported by electrochemical and spectroscopic measurements that suggest the presence of a less bulky *N*-substituent of the ^RN₃C⁻ ligand leads to a more accessible Ni^{III} center. These results also suggest that the (^{Np}N₃C)Ni system should be more reactive toward oxidation than the corresponding (^{tBu}N₃C)Ni and (^{pOMe}N₃C)Ni systems. Indeed, aerobic oxidative aromatic cyanation was achieved with the (^{Np}N₃C)Ni system at room temperature.

Introduction

Synthesis and characterization of organometallic high-valent Ni species is of great importance, as they have been widely proposed as key intermediates in carbon-carbon and carbon-heteroatom bond formation reactions.^{1–38} Starting more than three decades ago, extensive efforts have been devoted to synthesize such high-valent Ni species,^{39–50} however most of these isolated examples do not exhibit the expected bond formation reactivity. Recently, few examples of high-valent Ni species that undergo reductive elimination to form carbon-carbon and carbon-heteroatom bonds have been isolated and fully characterized.^{40,43,44,51–53} In these cases, ligand design turns out to play a vital role in determining the stability and reactivity of the corresponding Ni centers.

Our group has recently employed the pyridinophane-derived tetradentate ligand ^RN₃C⁻ (R = *tert*-butyl or neopentyl) to stabilize Ni^{III} centers and probe their bond formation reactivity such as aromatic methoxylation/hydroxylation,⁴³ aromatic cyanoalkylation,⁵² and aromatic cyanation⁵³ (Scheme 1). Based on these reports, ligand design was shown to have a dramatic effect on the reactivity of the Ni^{III} complexes. For



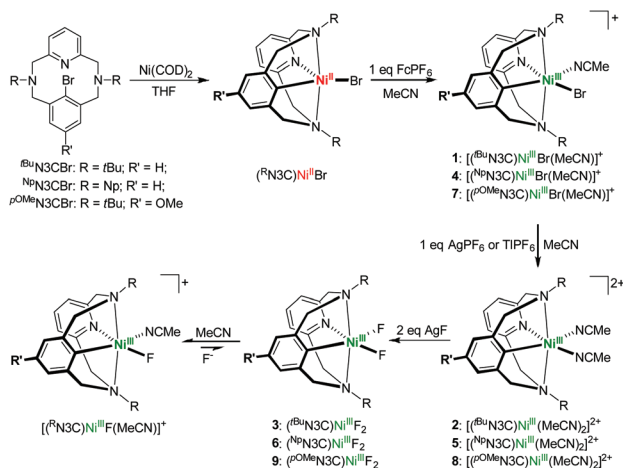
Scheme 1 Reactions mediated by high-valent (^RN₃C)Ni^{III} complexes, taken from (a) ref. 43, (b) ref. 53, and (c) ref. 52.

example, by substituting the *tert*-butyl (*t*Bu) groups with less sterically hindered neopentyl (Np) groups as the two amine *N*-substituents, the ^{Np}N₃C⁻ system exhibits enhanced C–H bond activation reactivity *versus* the ^{tBu}N₃C⁻ system.⁵² In this context, we set up to systematically investigate the effect of ligand modifications on the properties and reactivity of the corresponding Ni^{III} complexes. Herein, we compare the effects of three ligand systems. Thus, besides the ^{Np}N₃C⁻ and ^{tBu}N₃C⁻ ligands, we have designed the ^{pOMe}N₃C⁻ ligand by introducing a methoxy group in the *para* position of the phenyl C-donor group (Scheme 2). Electron paramagnetic

^aDepartment of Chemistry, Washington University, One Brookings Drive, St. Louis, Missouri 63130-4899, USA. E-mail: mirica@wustl.edu

^bDepartment of Chemistry and Biochemistry, University of Missouri-St. Louis, One University Boulevard, St. Louis, Missouri 63121-4400, USA

† Electronic supplementary information (ESI) available: Synthetic details, spectroscopic characterization, reactivity studies, and crystallographic data. CCDC 1458980 (3), 1458981 (7) and 1458982 (8). For ESI and crystallographic data in CIF or other electronic format see DOI: 10.1039/c6dt02185a



Scheme 2 Synthesis of $(\text{R}^{\text{N3C}})\text{Ni}^{\text{III}}$ complexes 1–9.

resonance (EPR) and cyclic voltammetry (CV) studies were employed to probe the electronic properties and redox behaviour of these $(\text{R}^{\text{N3C}})\text{Ni}$ complexes. Based on EPR and CV measurements, the modification of the substituents on the two amine donors affects the properties of Ni centers to a greater degree than the *para* substituents on the phenyl group, as shown also through structural characterization. In addition, the $\text{Ni}^{\text{II/III}}$ oxidation potentials the $(\text{R}^{\text{Np}}\text{N}_3\text{C})\text{Ni}$ complexes are dramatically lowered comparing to the $\text{tBu}_3\text{N}_3\text{C}^-$ and $\text{pOMe}_3\text{N}_3\text{C}^-$ analogs, and quantitative aerobically-induced aromatic cyanation using *t*BuNC at RT was achieved with the $(\text{R}^{\text{Np}}\text{N}_3\text{C})\text{Ni}$ system.

Experimental section

General specifications

All manipulations are carried out under an inert atmosphere using a nitrogen-filled glovebox or standard Schlenk techniques unless otherwise noted. All reagents for which synthesis is not given are commercially available from Sigma, Acros, STREM, VWR or TCI and were used as received without further purification. All glassware were oven or flame-dried immediately prior to use. Tetrahydrofuran, MeCN, *n*-pentane, and diethyl ether were degassed and dried by passage through a series of drying columns using an MBRAUN SPS Solvent System. All solvents were stored over 4 Å molecular sieves. Solvents were frequently tested using a standard solution of sodium benzophenone ketyl in THF to confirm the absence of moisture. Benzene-*d*₆ and MeCN-*d*₃ were degassed and dried over 4 Å molecular sieves before use. NMR spectra were recorded at ambient temperature unless otherwise stated on a Varian Mercury-300 300 MHz instrument. ¹H and ¹³C NMR chemical shifts are referenced to residual solvent and are reported in parts per million. Solution magnetic susceptibility measurements are obtained by the Evans method in MeCN using coaxial NMR tubes at 293 K, and diamagnetic corrections are applied as previously described.^{43,53} UV-vis spectra

were recorded on a Varian Cary 50 UV-vis spectrophotometer using Cary WinUV software. EPR spectra were recorded on a Bruker EMX-PLUS (9.2 GHz) or a JOEL JES-FA X-BAND (9.2 GHz) EPR spectrometer as a frozen glass at 77 K. ESI mass spectrometry (ESI-MS) studies were performed at the Washington University Mass Spectrometry Resource. Elemental microanalyses were performed by Intertek Pharmaceutical Services, Whitehouse, NJ.

Electrochemical measurements

Electrochemical grade *n*Bu₄NPF₆ was used as the supporting electrolyte. Cyclic voltammetry measurements were carried out in a glovebox under a dinitrogen atmosphere in a one-compartment cell using a CH Instruments electrochemical analyzer. A glassy carbon electrode and platinum wire were used as the working and auxiliary electrodes, respectively, and a Ag/AgCl wire was used as the pseudo reference electrode that was calibrated *vs.* Cp₂Fe.

Synthesis of Ni^{III} complexes

The synthesis of complexes 1, 2, and 4–6 was previously reported.^{43,52} 4-Bromo-3,5-bis(bromomethyl)anisole⁵⁴ and *N,N'*-(pyridine-2,6-diylbis(methylene))bis(2-methylpropan-2-amine)⁵⁵ were synthesized according to literature procedures. The $\text{pOMe}_3\text{N}_3\text{CBr}$ ligand was synthesized according to a reported procedure:⁴³ a 500 mL three-neck round bottom flask equipped with a reflux condenser, an addition funnel, and a magnetic stirring bar was charged with a solution of *N,N'*-(pyridine-2,6-diylbis(methylene))bis(2-methylpropan-2-amine) (0.54 g, 2.15 mmol, 1 equiv.) in 100 mL of toluene and 80 mL of 20% aqueous solution of Na₂CO₃. The stirred reaction mixture was pre-heated in an oil bath at 85 °C under N₂. A solution of 4-Bromo-3,5-bis(bromomethyl)anisole (0.80 g, 2.15 mmol, 1 equiv.) in 50 mL toluene was added dropwise to the stirred reaction mixture at 85 °C over 3 hours. The resulting solution was heated at 90 °C under N₂ for an additional 24 hours. The reaction mixture was cooled down to RT, the organic layer was separated, and the solvent was removed *in vacuo* to generate a yellowish oil mixture. The yellowish yellow oil was extracted with 20 mL of pentane/CH₂Cl₂ (4 : 1). The solution was concentrated to ~5 mL and stored at –20 °C overnight. Colorless crystals were obtained (yield: 200 mg, 20%). ¹H NMR (δ in ppm, C₆D₆, 293 K, 300 MHz): 7.00 (t, 1H, Ar), 6.73 (d, 2H, Ar), 6.57 (s, 2H, Ar), 4.37 (d, 2H, CH₂), 4.02–3.80 (m, 6H, CH₂), 3.27 (s, 3H, CH₃), 1.10 (s, 18H, CH₃). ¹³C NMR (δ in ppm, C₆D₆, 293 K, 100.5 MHz): 161.3, 158.4, 140.9, 134.6, 121.9, 118.3, 111.0, 57.7, 56.2, 55.5, 55.3, 28.3. ESI-MS of $\text{pOMe}_3\text{N}_3\text{CBr}$ in MeCN: *m/z* 460.1961 (calcd for $[\text{pOMe}_3\text{N}_3\text{CBrH}]^+$, C₂₄H₃₅BrON₃, *m/z* 460.1964).

Synthesis of $(\text{tBu}_3\text{N}_3\text{C})\text{Ni}^{\text{III}}\text{F}_2$ (3). To a solution of 2 (17.8 mg, 0.023 mmol, 1 equiv.) in 1.5 mL MeCN, AgF (6.5 mg, 0.046 mmol, 2.2 equiv.) was added at RT. The reaction was stirred overnight, during which the green solution turned red. The formed precipitates were removed by filtration and the filtrate was layered with Et₂O and stored at –35 °C. Dark red crystals of X-ray quality formed after 2 days (yield: 6.3 mg,

62%). ^{19}F NMR (δ in ppm, CD_3CN , 293 K, 300 MHz): -35.9 (br, 1F). Evans' method (CD_3CN): $\mu_{\text{eff}} = 1.84\mu_{\text{B}}$. ESI-MS of ($^t\text{BuN}_3\text{C}$) $\text{Ni}^{\text{III}}\text{F}_2$ in CH_3CN : m/z 427.1930 (calcd for [$^t\text{BuN}_3\text{C}$] $\text{Ni}^{\text{III}}\text{F}_2^+$, $\text{C}_{23}\text{H}_{32}\text{NiFN}_3$, m/z 427.1934). UV-vis (CH_3CN) λ_{max} (nm) (ϵ [$\text{mol}^{-1}\text{cm}^{-1}$]): 296 (1831), 331 (1016), 382 (535), 471 (281), 562 (165). Elemental analysis of ($^t\text{BuN}_3\text{C}$) $\text{Ni}^{\text{III}}\text{F}_2\cdot\text{H}_2\text{O}$: calcd for $\text{C}_{23}\text{H}_{36}\text{F}_2\text{N}_3\text{NiO}_2$: C, 57.17; H, 7.51; N, 8.70; found: C, 56.51; H, 7.13; N, 8.21.

Synthesis of ($^p\text{OMeN}_3\text{C}$) $\text{Ni}^{\text{II}}\text{Br}$ (9). To a solution of $^p\text{OMeN}_3\text{CBr}$ (47.0 mg, 0.102 mmol, 1 equiv.) in 2 mL of THF, $\text{Ni}(\text{COD})_2$ (28.5 mg, 0.102 mmol, 1 equiv.) was added at -35°C . The reaction was stirred at -35°C overnight. A filtration was applied to remove a black solid. The reaction was concentrated to 1 mL under vacuum. To this reaction, 10 mL of pentane was added and the product was crashed out as a reddish solid. The product was washed with pentane (3×1 mL) and dried under vacuum. This product was used without further purification due to its air sensitivity (yield: 35.5 mg, 67%).

Synthesis of [$^p\text{OMeN}_3\text{C}$] $\text{Ni}^{\text{III}}(\text{MeCN})\text{BrPF}_6$ (7). To a solution of ($^p\text{OMeN}_3\text{C}$) $\text{Ni}^{\text{II}}\text{Br}$ (29.2 mg, 0.056 mmol, 1 equiv.) in 2 mL of CH_3CN , FcPF_6 (18.6 mg, 0.056 mmol, 1 equiv.) was added at RT. The reaction was stirred overnight. A filtration was applied to remove any solid and the solvent was removed by vacuum. The solid was washed by Et_2O and then was dissolved into 1.5 mL of CH_3CN . Dark red X-ray quality crystals of [$^p\text{OMeN}_3\text{C}$] $\text{Ni}^{\text{III}}(\text{MeCN})\text{BrPF}_6$ were grown by layering with Et_2O overnight (yield: 24.2 mg, 61%). ^{19}F NMR (δ in ppm, CD_3CN , 293 K, 300 MHz): -35.9 (br, 1F). Evans' method (CD_3CN): $\mu_{\text{eff}} = 1.72\mu_{\text{B}}$. ESI-MS of [$^p\text{OMeN}_3\text{C}$] $\text{Ni}^{\text{III}}(\text{MeCN})\text{BrPF}_6$ in CH_3CN : m/z 517.1226 (calcd for [$^p\text{OMeN}_3\text{C}$] $\text{Ni}^{\text{III}}\text{Br}$), $\text{C}_{24}\text{H}_{34}\text{NiBrN}_3\text{O}$, m/z 517.1233). UV-vis (CH_3CN) λ_{max} (nm) (ϵ [$\text{mol}^{-1}\text{cm}^{-1}$]): 292 (1186), 375 (365), 580 (67). Elemental analysis of [$^p\text{OMeN}_3\text{C}$] $\text{Ni}^{\text{III}}(\text{MeCN})\text{BrPF}_6$: calcd for $\text{C}_{26}\text{H}_{37}\text{BrF}_6\text{N}_4\text{NiOP}$: C, 44.29; H, 5.29; N, 7.95; found: C, 44.13; H, 5.33; N, 7.93.

Synthesis of [$^p\text{OMeN}_3\text{C}$] $\text{Ni}^{\text{III}}(\text{MeCN})_2(\text{SbF}_6)_2$ (8). To a solution of 7 (14.3 mg, 0.020 mmol, 1 equiv.) in 1.5 mL MeCN, AgSbF_6 (7.8 mg, 0.023 mmol, 1.1 equiv.) was added at RT. The reaction was stirred for an hour, the formed precipitates were removed by filtration, and the filtrate was layered with Et_2O . Dark green crystals of X-ray quality formed after 2 days at RT (yield: 19.6 mg, 97%). ^{19}F NMR (δ in ppm, CD_3CN , 293 K, 300 MHz): -109 (m, 12F, SbF_6). Evans' method (CD_3CN): $\mu_{\text{eff}} = 1.73\mu_{\text{B}}$. UV-vis (CH_3CN) λ_{max} (nm) (ϵ [$\text{mol}^{-1}\text{cm}^{-1}$]): 233 (654), 266 (381), 315 (142), 389 (26). Elemental analysis of [$^p\text{OMeN}_3\text{C}$] $\text{Ni}^{\text{III}}(\text{MeCN})_2(\text{SbF}_6)_2$: calcd for $\text{C}_{28}\text{H}_{40}\text{F}_{12}\text{N}_5\text{NiOSb}_2$: C, 33.87; H, 4.06; N, 7.05; found: C, 33.41; H, 3.95; N, 6.76.

Synthesis of ($^p\text{OMeN}_3\text{C}$) $\text{Ni}^{\text{III}}\text{F}_2$ (9). To a solution of 8 (30.3 mg, 0.030 mmol, 1 equiv.) in 2 mL MeCN, AgF (8.9 mg, 0.066 mmol, 2.2 equiv.) was added at room temperature. The reaction was stirred overnight, during which the green solution turned red. The formed precipitates were removed by filtration and the filtrate was layered with Et_2O and stored at -35°C . Dark red crystals formed after 2 days (yield: 7.2 mg, 51%). The crystals turned out to be twinning and failed to provide good diffraction data even after several attempts. ^{19}F NMR (δ in ppm, CD_3CN , 293 K, 300 MHz): -34.9 (br, 1F). Evans' method

(CD_3CN): $\mu_{\text{eff}} = 1.82\mu_{\text{B}}$. ESI-MS of ($^p\text{OMeN}_3\text{C}$) $\text{Ni}^{\text{III}}\text{F}_2$ in CH_3CN : m/z 457.2023 (calcd for [$^p\text{OMeN}_3\text{C}$] $\text{Ni}^{\text{III}}\text{F}_2^+$, $\text{C}_{24}\text{H}_{34}\text{NiFN}_3\text{O}$, m/z 457.2030). UV-vis (CH_3CN) λ_{max} (nm) (ϵ [$\text{mol}^{-1}\text{cm}^{-1}$]): 233 (1438), 267 (878), 293 (536), 330 (189). Elemental analysis of ($^p\text{OMeN}_3\text{C}$) $\text{Ni}^{\text{III}}\text{F}_2\cdot\text{MeCN}\cdot\text{H}_2\text{O}$: calcd for $\text{C}_{26}\text{H}_{39}\text{F}_2\text{N}_4\text{NiO}_2$: C, 58.23; H, 7.33; N, 10.45; found: C, 58.05; H, 6.84; N, 10.42.

Synthesis of ($^n\text{P}_3\text{N}_3\text{C}$) $\text{Ni}^{\text{II}}\text{Br}$ (10). To a solution of $^n\text{P}_3\text{N}_3\text{CBr}$ (50.5 mg, 0.110 mmol, 1 equiv.) in 2 mL THF, $\text{Ni}(\text{COD})_2$ (31.0 mg, 0.110 mmol, 1 equiv.) was added at -35°C and the reaction was stirred overnight. A filtration was applied to remove a black precipitate and the reaction was concentrated to 1 mL under vacuum. To this reaction, 10 mL of pentane was added and the product was crashed out as a reddish solid. The product was washed with pentane (3×1 mL) and dried under vacuum. This product was used without further purification due to its air sensitivity (yield: 39 mg, 68%).

Synthesis of [$^n\text{P}_3\text{N}_3\text{C}$] $\text{Ni}^{\text{II}}(\text{MeCN})_2\text{PF}_6$ (11). To a solution of 10 (24.4 mg, 0.047 mmol, 1 equiv.) in 1 mL of CH_3CN , TiPF_6 (17.5 mg, 0.050 mmol, 1.05 equiv.) was added at RT. The reaction was stirred for 1 hour and the white TiBr precipitate was removed by filtration. The reaction was concentrated to 1 mL under vacuum. To this reaction, 10 mL of Et_2O was added and the product was crashed out as a reddish solid. The product was washed with Et_2O (3×1 mL) and dried under vacuum. This product was used without further purification due to its air sensitivity (yield: 28 mg, 90%).

General procedure for the aerobic aromatic cyanation reactions

To a solution of Ni^{II} precursor (1 equiv.) in MeCN or CD_3CN , 1 equiv. $t\text{BuNC}$ was added. The reaction mixture was stirred for 5 min at RT and then brought out from the glovebox and exposed to air. The red solution turned colourless within 5 min. The reaction was monitored by ^1H NMR and ESI-MS and the quantitative generation of $^t\text{BuN}_3\text{CCN}$ is observed. The solvent was removed under vacuum, and the solid was washed with Et_2O (3×1 mL) and dried under vacuum. See ESI† for detailed experimental procedures.

Results and discussion

Synthesis and characterization of complexes 1–9

The Ni^{II} precursors ($^t\text{BuN}_3\text{C}$) $\text{Ni}^{\text{II}}\text{Br}$, ($^n\text{P}_3\text{N}_3\text{C}$) $\text{Ni}^{\text{II}}\text{Br}$ (10), and ($^p\text{OMeN}_3\text{C}$) $\text{Ni}^{\text{II}}\text{Br}$ were prepared following previously published literature procedures (Scheme 2).^{43,52,53} These Ni^{II} complexes can each be oxidized with 1 equiv. of FcPF_6 to generate the corresponding Ni^{III} complexes [$^t\text{BuN}_3\text{C}$] $\text{Ni}^{\text{III}}\text{Br}(\text{MeCN})\text{PF}_6$ (1), [$^n\text{P}_3\text{N}_3\text{C}$] $\text{Ni}^{\text{III}}\text{Br}(\text{MeCN})\text{PF}_6$ (4), and [$^p\text{OMeN}_3\text{C}$] $\text{Ni}^{\text{III}}\text{Br}(\text{MeCN})\text{PF}_6$ (7) at RT. The solid state structures of complexes 1, 4, and 7 reveal the Ni^{III} centers adopt distorted octahedral geometry as expected for d^7 ions, with the amine donors in the axial positions (Fig. 1). Based on the Evans method, the Ni^{III} complexes 1, 4 and 7 are paramagnetic and exhibit effective magnetic moments μ_{eff} of 1.68, 1.74 and $1.72\mu_{\text{B}}$ at 298 K, corresponding to one unpaired electron. Their EPR spectra (77 K, PrCN glass) reveal rhombic signals (Fig. 2) with g_{ave}

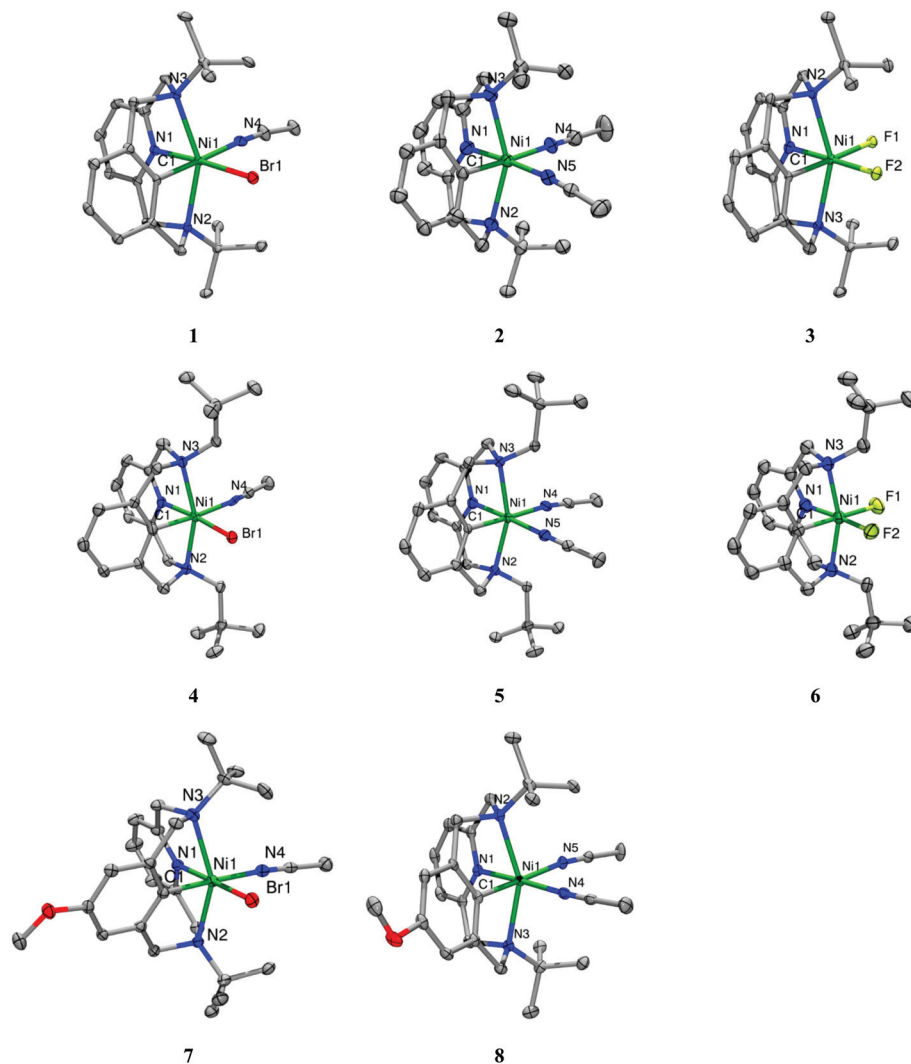


Fig. 1 ORTEP representation (50% probability thermal ellipsoids) of 1–8. For clarity, hydrogen atoms have been omitted. Selected bond distances (Å): 1: Ni1–C1, 1.887(1); Ni1–N1, 1.948(1); Ni1–N2, 2.312(1); Ni1–N3, 2.291(1); Ni1–Br1, 2.390(1); Ni1–N4, 2.009(1). 2: Ni1–C1, 1.902(1); Ni1–N1, 1.929(1); Ni1–N2, 2.273(1); Ni1–N3, 2.259(1); Ni1–N4, 2.004(1); Ni1–N5, 1.980(1). 3: Ni1–C1, 1.888(2); Ni1–N1, 1.900(2); Ni1–N2, 2.256(2); Ni1–N3, 2.283(2); Ni1–F1, 1.926(1); Ni1–F2, 1.912(1). 4: Ni1–C1, 1.911(3); Ni1–N1, 1.938(3); Ni1–N2, 2.239(3); Ni1–N3, 2.238(3); Ni1–N4, 2.061(2); Ni1–Br1, 2.373(1). 5: Ni1–C1, 1.900(2); Ni1–N1, 1.901(2); Ni1–N2, 2.196(2); Ni1–N3, 2.213(2); Ni1–N4, 1.993(2); Ni1–N5, 1.959(2). 6: Ni1–C1, 1.886(4); Ni1–N1, 1.904(4); Ni1–N2, 2.185(4); Ni1–N3, 2.162(3); Ni1–F1, 1.916(2); Ni1–F2, 1.932(3). 7: Ni1–C1, 1.895(3); Ni1–N1, 1.961(2); Ni1–N2, 2.300(2); Ni1–N3, 2.333(2); Ni1–Br1, 2.399(1); Ni1–N4, 2.006(2). 8: Ni1–C1, 1.889(3); Ni1–N1, 1.912(2); Ni1–N2, 2.237(2); Ni1–N3, 2.243(2); Ni1–N4, 1.961(12); Ni1–N5, 2.007(2).

values of 2.145 for **1**, 2.132 for **4** and 2.147 for **7** (Table 1). In addition, superhyperfine coupling to the two axial N donors ($I = 1$) is observed in the g_z direction and superhyperfine coupling to the Br atom ($I = 3/2$) is observed along the g_y and g_z directions. Taken together, the observed structural and EPR parameters for complexes **1**, **4**, and **7** strongly suggest the presence of a distorted octahedral Ni^{III} d⁷ center with a d_{z²} ground state.

When complexes **1**, **4**, and **7** were treated with 1 equiv. of AgPF₆ or TlPF₆ at RT, the corresponding Ni^{III} complexes [(^tBuN₃C)Ni^{III}(MeCN)₂](PF₆)₂ (**2**), [(^NP⁺N₃C)Ni^{III}(MeCN)₂](PF₆)₂ (**5**) and [(^pOMeN₃C)Ni^{III}(MeCN)₂](PF₆)₂ (**8**) were obtained in very good yields (Scheme 1). The solid state structures of complexes **2**, **5**, and **8** reveal the Ni^{III} centers adopt distorted octahedral

geometry as expected for d⁷ ions, with the amine donors in the axial positions (Fig. 1). Complexes **2**, **5** and **8** are indeed paramagnetic with effective magnetic moments μ_{eff} of 1.71, 1.71 and 1.73 μ_B at 298 K, corresponding to one unpaired electron. Their EPR spectra (77 K, PrCN glass) reveal rhombic signals (Fig. 2) with g_{ave} values of 2.127 for **2**, 2.118 for **5** and 2.129 for **8** (Table 1). In addition, superhyperfine coupling to the two axial N donors ($I = 1$) is observed in the g_z direction, however no superhyperfine coupling is observed along the g_y and g_z directions, supporting the bromine abstraction by the Ag⁺ or Tl⁺ ions. Taken together, the observed structural and EPR parameters for complexes **2**, **5** and **8** suggest the generation of the dicationic Ni^{III}-disolvento complexes. Surprisingly, complexes **2**, **5**, and **8** are all air-stable at RT.

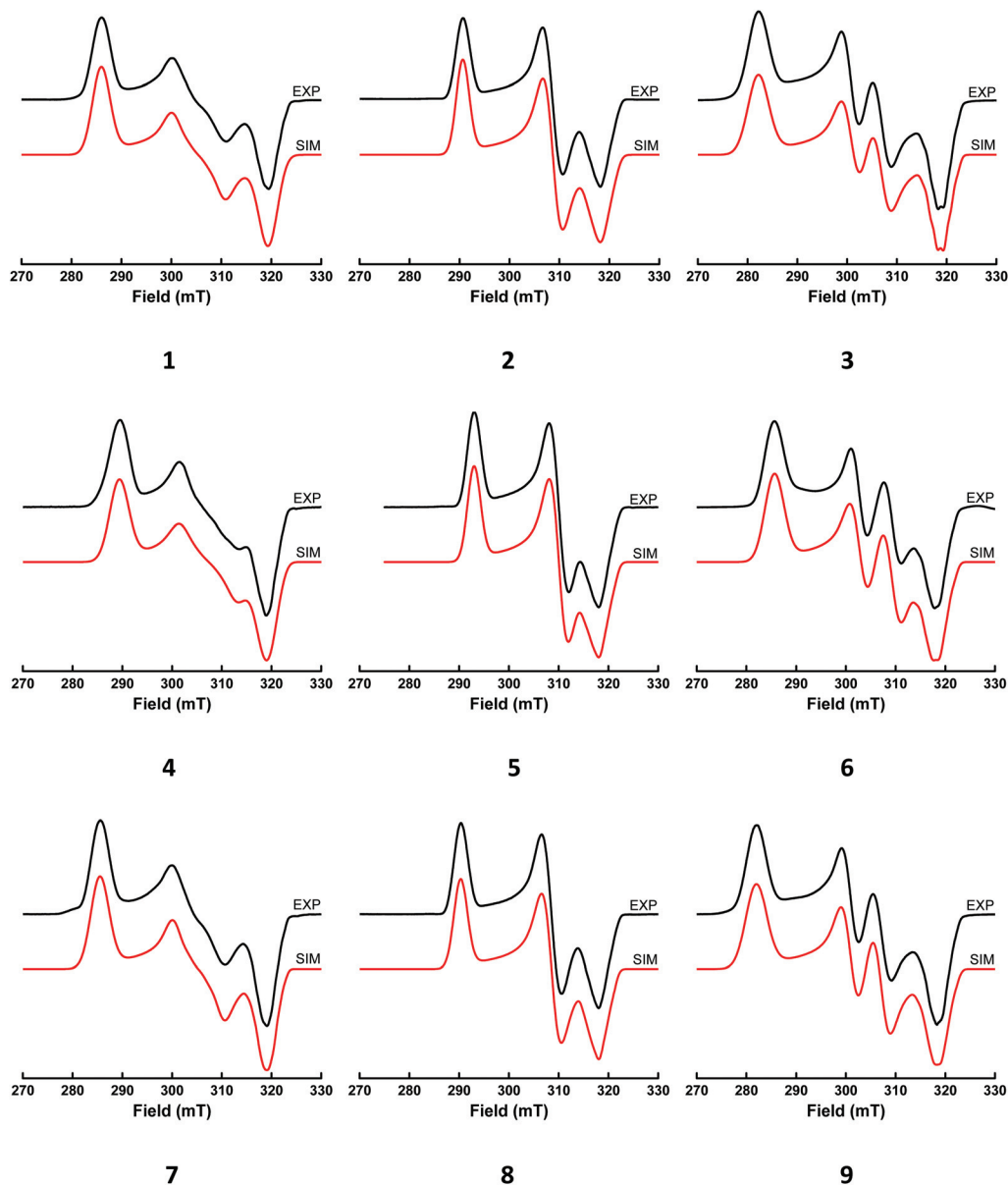


Fig. 2 The experimental and simulated EPR spectra of 1–9 in nPrCN at 77 K. Simulation using the following parameters: **1**, $g_x = 2.272$; $g_y = 2.128$ ($A_{Br} = 26.5$ G); $g_z = 2.035$ ($A_{2N} = 10.0$ G, $A_{Br} = 5.0$ G); **2**, $g_x = 2.236$; $g_y = 2.105$; $g_z = 2.041$ ($A_{2N} = 13.5$ G); **3**, $g_x = 2.303$; $g_y = 2.139$ ($A_F = 60.0$ G); $g_z = 2.039$ ($A_{2N} = 13.0$ G, $A_F = 13.0$ G); **4**, $g_x = 2.244$; $g_y = 2.115$ ($A_{Br} = 29.0$ G); $g_z = 2.037$ ($A_{2N} = 12.0$ G, $A_{Br} = 6.0$ G); **5**, $g_x = 2.217$; $g_y = 2.095$; $g_z = 2.041$ ($A_{2N} = 14.0$ G); **6**, $g_x = 2.274$; $g_y = 2.124$ ($A_F = 65.0$ G); $g_z = 2.043$ ($A_{2N} = 13.5$ G, $A_F = 17.5$ G); **7**, $g_x = 2.276$; $g_y = 2.128$ ($A_{Br} = 26.0$ G); $g_z = 2.037$ ($A_{2N} = 11.0$ G, $A_{Br} = 9.0$ G); **8**, $g_x = 2.238$; $g_y = 2.106$; $g_z = 2.042$ ($A_{2N} = 13.5$ G); **9**, $g_x = 2.304$; $g_y = 2.138$ ($A_F = 62.0$ G); $g_z = 2.035$ ($A_{2N} = 13.5$ G, $A_F = 17.0$ G).

Table 1 Spectroscopic and structural comparison of (R N3C)Ni^{III} complexes (ND = not determined)

Ligands complexes	t BuN3C ⁻			n PrN3C ⁻			p OMeN3C ⁻		
	1	2	3	4	5	6	7	8	9
Ni ^{III} (mV)	-650	-560	-950	-940	-750	-1080	-720	-700	-1040
EPR (g_{ave})	2.145	2.127	2.160	2.132	2.118	2.147	2.147	2.129	2.159
Ni1–N _{amine} (Å)	2.302	2.266	2.270	2.239	2.205	2.174	2.317	2.240	ND
Ni1–C1 (Å)	1.887	1.902	1.888	1.911	1.900	1.886	1.895	1.889	ND

Since the Ni^{III}-disolvento complexes **2**, **5**, and **8** have two *cis* coordination sites available for exogenous ligands, we set out to introduce F⁻ to coordinate to the Ni^{III} centers. By reacting complexes **2**, **5** and **8** with 2 equiv. of AgF at RT, complexes (^tBuN₃C)Ni^{III}F₂ (**3**), (^{Np}N₃C)Ni^{III}F₂ (**6**), and (^pOMeN₃C)Ni^{III}F₂ (**9**) were generated. Structural characterization of **3** and **6** reveals Ni^{III} centers with distorted octahedral geometries and the amine donors in the axial positions, while the two F⁻ ions occupy the two *cis* coordination sites (Fig. 1). Complexes **3**, **6** and **9** exhibit effective magnetic moments μ_{eff} of 1.84, 1.77 and 1.82 μ_{B} at 298 K, corresponding to one unpaired electron. Their EPR characterization (77 K, PrCN glass) shows the presence of rhombic signals (Fig. 2) with g_{ave} values of 2.160 for **3**, 2.147 for **6** and 2.159 for **9** (Table 1), along with superhyperfine coupling to the two axial N donors ($I = 1$) is observed in the g_z direction for all three complexes. Interestingly, the EPR spectra of **3**, **6** and **9** are best simulated using superhyperfine coupling in the g_y and g_z directions to only one F⁻ ion ($I = 1/2$) (Fig. 2). Overall, the observed structural and EPR parameters strongly suggest the existence of complexes **3**, **6** and **9** as difluoride Ni^{III} complexes, in the solid state and as monofluoride Ni^{III} complexes [(^RN₃C)Ni^{III}F(MeCN)]⁺ in MeCN. Importantly, **3**, **6** and **9** are the first isolated high-valent organometallic Ni–F complexes,⁵² although such species have recently been proposed as intermediates in oxidatively-induced C–F bond formation.⁵⁶

Ligand effect on the properties of Ni^{III} complexes

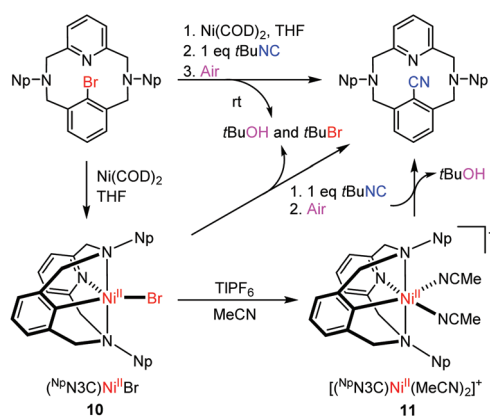
With these fully characterized Ni^{III} complexes in hand, we were able to establish a relationship between their structural parameters their electronic properties as exhibited in their EPR parameters (Fig. 2 and Table 1) and their Ni^{III/II} redox potentials (Table 1). For example, in the EPR spectra the ordering of the g_{ave} values: 2.160 for **3** > 2.145 for **1** > 2.127 for **2** is as expected when replacing weakly back-bonding MeCN ligands with stronger σ -donor and π -donor bromide or fluoride ligands. This ordering is also true for the Ni^{III/II} redox potentials: –950 mv for **3** < –650 mv for **1** < –560 mv for **2**, indicating the largest electron density at the Ni^{III} center for **3**, followed by **1** and then **2** (Table 1), and similar trends are observed in both ^{Np}N₃C⁻ and ^pOMeN₃C⁻ systems as well. In addition, based on the superhyperfine coupling pattern, the presence of exogenous ligands such as fluoride, bromide, and MeCN can be easily identified based on the simulated EPR spectra that include corresponding superhyperfine coupling constants (Fig. 2). This provides a rapid method to confirm if an anion (e.g., a nucleophile) is interacting with the Ni^{III} center or not.

Zargarian *et al.* have reported that modification of the side-arms of ‘ECE’ pincer ligand systems (where E is an L-type donor and C is the *ipso*-carbon of the phenyl ring) can dramatically impact the properties of the corresponding Ni^{II} complexes.^{41,42,57,58} Inspired by this elegant work, we developed the ^{Np}N₃C⁻ ligand by substituting the *tert*-butyl groups (*t*Bu) with less sterically hindered neopentyl groups (Np) as the two amine *N*-substituents (Scheme 2). As expected, the two amine

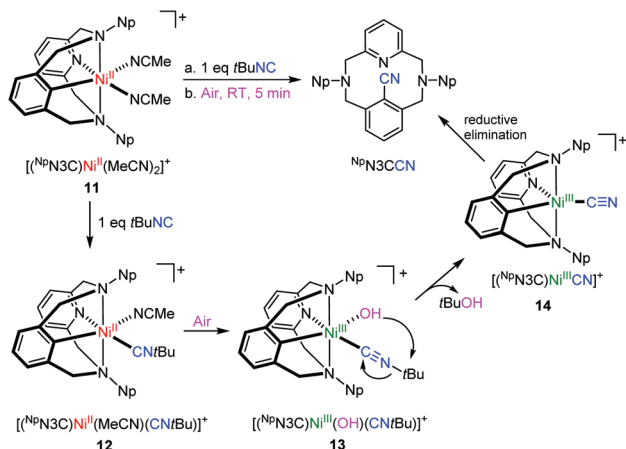
donors interact more strongly with the Ni^{III} center in the ^{Np}N₃C⁻ system vs. the ^tBuN₃C⁻ system, evidenced by the shorter average Ni–N_{amine} bond distances in **1** vs. **4**, **2** vs. **5**, and **3** vs. **6** (Fig. 1 and Table 1). Moreover, the stronger Ni–amine interactions lead to larger superhyperfine coupling constants for the g_z values in the EPR spectra of **1** vs. **4**, **2** vs. **5**, and **3** vs. **6** (Fig. 2). Finally, the Ni^{III/II} redox potentials for the ^{Np}N₃C⁻ system are lowered by 150–300 mV compared to those of the ^tBuN₃C⁻ system, which will have a dramatic effect on their reactivity (see below). Interestingly, for the ^pOMeN₃C⁻ system, no significant changes in metrical parameters are observed for the corresponding Ni^{III} centers vs. those supported by the ^tBuN₃C⁻ system, while the Ni^{III/II} redox potentials are lowered by less than 100 mV, most likely due to the slightly increased electron donating ability of the phenyl ring in the ^pOMeN₃C⁻ ligand system. Overall, these comparisons suggest that modification of the two amine side-arms of the ^RN₃C⁻ systems impacts the most the properties of the Ni^{III} centers, similar to was observed for Ni^{II} complexes by Zargarian *et al.*^{41,42,57,58}

Aerobically-induced aromatic cyanation mediated by Ni^{III}

Recently, we have reported the oxidatively-induced aromatic cyanation reactivity of the ^tBuN₃CNi system.⁵³ Since the ^{Np}N₃CNi systems exhibit dramatically lowered Ni^{III/II} redox potentials (Table 1), we sought out to test whether even milder oxidants could promote the aromatic cyanation reaction. For that, the complex [(^{Np}N₃C)Ni^{II}(MeCN)₂]PF₆, **11**, was synthesized by reacting **11** with 1 equiv. TlPF₆. Gratifyingly, when **11** was reacted with 1 equiv. *t*BuNC and then exposed to air for 5 min, the quantitative generation of the cyanation product ^{Np}N₃CCN was observed (Scheme 3). Monitoring of the reaction by NMR in CD₃CN reveals the formation of *t*BuOH as a by-product (Scheme 4). Alternatively, when complex (^{Np}N₃C)Ni^{II}Br, **10**, was mixed with 1 equiv. of *t*BuNC and then stirred in air for 5 min, ^{Np}N₃CCN was also generated quantitatively. In this case both *t*BuOH and *t*BuBr are observed by ¹H NMR in ~1 : 1 ratio (Fig. S2†). The aromatic cyanation can also be achieved in



Scheme 3 Aerobically-induced aromatic cyanation using *t*BuNC as the cyanide source.



Scheme 4 Proposed mechanism of aerobically-induced aromatic cyanation mediated by Ni^{III} , including proposed intermediates **12**–**14**.

a one pot reaction, starting with NpN_3CBr and $\text{Ni}(\text{COD})_2$, followed by addition of *t*BuNC and air, to generate NpN_3CCN in 50% unoptimized yield. A possible mechanism is provided based on the observed aerobic reaction of **11** with *t*BuNC (Scheme 4). When 1 equiv. *t*BuNC is added to **11**, the intermediate $[(^{\text{Np}}\text{N}_3\text{C})\text{Ni}^{\text{II}}(\text{MeCN})(\text{CN}t\text{Bu})]^+$, **12**, is likely generated, which can be oxidized by air to the proposed intermediate $[(^{\text{Np}}\text{N}_3\text{C})\text{Ni}^{\text{III}}(\text{OH})(\text{CN}t\text{Bu})]^+$, **13**. Species **13** then undergoes rapid heterolytic cleavage of the N-*t*Bu bond to generate a cyanide Ni^{III} complex $[(^{\text{Np}}\text{N}_3\text{C})\text{Ni}^{\text{III}}\text{CN}]^+$, **14**; similar heterolytic *t*BuNC cleavage has been mediated by transition metal complexes have been observed before.^{53,59–62} Finally, the cyanation product NpN_3CCN can be generated through reductive elimination from **14**. It is important to note that while a Ni^{I} product is expected to form upon the reductive elimination step, such a species could not be detected, most likely due to its rapid oxidation to Ni^{II} under aerobic conditions.

In order to provide support for this proposed mechanism, a mixture of **11** and 1 equiv. of $\text{CN}t\text{Bu}$ was monitored by ^1H NMR in the absence of an oxidant. No cyanation product was observed at RT for 24 hours, indicating this cyanation process does not occur at the Ni^{II} stage. Furthermore, when **5** is reacted with 1 equiv. of *t*BuNC, quantitative generation of NpN_3CCN is observed within 5 min. Monitoring of this reaction by EPR revealed a rapid disappearance of the EPR signal of **5** upon addition of *t*BuNC is added, further suggesting that the cyanation reaction occurs at Ni^{III} . These results further support that the cyanation reaction is oxidatively-induced and a proposed Ni^{III} intermediate **13** is likely involved. When **5** is reacted with KCN, the generation of NpN_3CCN is also observed, further supporting the heterolytic cleavage of *t*BuNC the likely involvement of intermediate **14**. By comparison, the $t\text{BuN}_3\text{CNi}^{\text{II}}$ complexes cannot undergo aerobically-induced cyanation, likely due to their higher $\text{Ni}^{\text{III/II}}$ redox potentials (Table 1), and stronger oxidants are needed for this reaction to proceed.⁵³ When the corresponding $p\text{OMeN}_3\text{CNi}$ complexes, which are slightly more electron rich than the $t\text{BuN}_3\text{C}^-$ analogues, were

exposed to air in presence of *t*BuNC, the cyanation product $p\text{OMeN}_3\text{CCN}$ can be observed by ESI-MS (m/z 407.2802, calcd for $[p\text{OMeN}_3\text{CCN}\cdot\text{H}]^+$, $\text{C}_{25}\text{H}_{35}\text{N}_4\text{O}$: 407.2805) and NMR. However, due to the introduction of the *p*-methoxy group, the electron rich phenyl ring undergoes unwanted side reactions under air that dramatically reduced the yield of the cyanation product (Fig. S3†).

Conclusions

In conclusion, a series of Ni^{III} complexes supported by $\text{R}^{\text{N}}\text{N}_3\text{C}^-$ ligands were synthesized and fully characterized. Based on structural data and EPR and CV studies, modification of the substituents on the two amine N-donors plays a greater role in modulating the properties of the Ni^{III} centers than changing the *para* substituents of the phenyl C-donor group. Furthermore, rapid and quantitative aerobically-induced aromatic cyanation was accomplished by employing $p\text{OMeN}_3\text{CNi}$ complexes that exhibit dramatically lowered $\text{Ni}^{\text{III/II}}$ redox potentials. Overall, these studies should provide insight into the development of Ni-mediated organometallic reactions that involve Ni^{III} intermediates, including exceedingly rare aerobically-induced transformations.

Acknowledgements

We thank the National Science Foundation (CHE-1255424) for support. The purchase of the Bruker EMX-PLUS EPR spectrometer was supported by the National Science Foundation (MRI, CHE-1429711).

Notes and references

- 1 T. T. Tsou and J. K. Kochi, *J. Am. Chem. Soc.*, 1978, **100**, 1634.
- 2 T. T. Tsou and J. K. Kochi, *J. Am. Chem. Soc.*, 1979, **101**, 7547.
- 3 C. Amatore and A. Jutand, *Organometallics*, 1988, **7**, 2203.
- 4 J. Zhou and G. C. Fu, *J. Am. Chem. Soc.*, 2004, **126**, 1340.
- 5 D. A. Powell and G. C. Fu, *J. Am. Chem. Soc.*, 2004, **126**, 7788.
- 6 N. A. Owston and G. C. Fu, *J. Am. Chem. Soc.*, 2010, **132**, 11908.
- 7 S. L. Zultanski and G. C. Fu, *J. Am. Chem. Soc.*, 2011, **133**, 15362.
- 8 A. S. Dudnik and G. C. Fu, *J. Am. Chem. Soc.*, 2012, **134**, 10693.
- 9 S. L. Zultanski and G. C. Fu, *J. Am. Chem. Soc.*, 2013, **135**, 624.
- 10 G. D. Jones, C. McFarland, T. J. Anderson and D. A. Vivic, *Chem. Commun.*, 2005, 4211.
- 11 G. D. Jones, J. L. Martin, C. McFarland, O. R. Allen, R. E. Hall, A. D. Haley, R. J. Brandon, T. Konovalova,

- P. J. Desrochers, P. Pulay and D. A. Vicic, *J. Am. Chem. Soc.*, 2006, **128**, 13175.
- 12 V. B. Phapale, E. Bunuel, M. Garcia-Iglesias and D. J. Cardenas, *Angew. Chem., Int. Ed.*, 2007, **46**, 8790.
- 13 V. B. Phapale, M. Guisan-Ceinos, E. Bunuel and D. J. Cardenas, *Chem. – Eur. J.*, 2009, **15**, 12681.
- 14 H. G. Gong and M. R. Gagné, *J. Am. Chem. Soc.*, 2008, **130**, 12177.
- 15 H. G. Gong, R. S. Andrews, J. L. Zuccarello, S. J. Lee and M. R. Gagné, *Org. Lett.*, 2009, **11**, 879.
- 16 O. Vechorkin and X. Hu, *Angew. Chem., Int. Ed.*, 2009, **48**, 937.
- 17 O. Vechorkin, V. r. Proust and X. Hu, *J. Am. Chem. Soc.*, 2009, **131**, 9756.
- 18 X. Hu, *Chem. Sci.*, 2011, **2**, 1867.
- 19 D. A. Everson, R. Shrestha and D. J. Weix, *J. Am. Chem. Soc.*, 2010, **132**, 920.
- 20 S. Biswas and D. J. Weix, *J. Am. Chem. Soc.*, 2013, **135**, 16192.
- 21 A. Joshi-Pangu, C. Y. Wang and M. R. Biscoe, *J. Am. Chem. Soc.*, 2011, **133**, 8478.
- 22 X. L. Yu, T. Yang, S. L. Wang, H. L. Xu and H. G. Gong, *Org. Lett.*, 2011, **13**, 2138.
- 23 Y. J. Dai, F. Wu, Z. H. Zang, H. Z. You and H. G. Gong, *Chem. – Eur. J.*, 2012, **18**, 808.
- 24 H. Xu, C. Zhao, Q. Qian, W. Deng and H. Gong, *Chem. Sci.*, 2013, **4**, 4022.
- 25 K. Koo and G. L. Hillhouse, *Organometallics*, 1995, **14**, 4421.
- 26 K. M. Koo, G. L. Hillhouse and A. L. Rheingold, *Organometallics*, 1995, **14**, 456.
- 27 R. Y. Han and G. L. Hillhouse, *J. Am. Chem. Soc.*, 1997, **119**, 8135.
- 28 B. L. Lin, C. R. Clough and G. L. Hillhouse, *J. Am. Chem. Soc.*, 2002, **124**, 2890.
- 29 J. Breitenfeld, J. Ruiz, M. D. Wodrich and X. Hu, *J. Am. Chem. Soc.*, 2013, **135**, 12004.
- 30 M. I. Lipschutz and T. D. Tilley, *Angew. Chem., Int. Ed.*, 2014, **53**, 7290.
- 31 A. N. Vedernikov, *ChemCatChem*, 2014, **6**, 2490.
- 32 G. T. Venkanna, H. D. Arman and Z. J. Tonzetich, *ACS Catal.*, 2014, **4**, 2941.
- 33 J. Breitenfeld, M. D. Wodrich and X. Hu, *Organometallics*, 2014, **33**, 5708.
- 34 N. D. Schley and G. C. Fu, *J. Am. Chem. Soc.*, 2014, **136**, 16588.
- 35 Y. Zhao and D. J. Weix, *J. Am. Chem. Soc.*, 2015, **137**, 3237.
- 36 J. Cornella, J. T. Edwards, T. Qin, S. Kawamura, J. Wang, C. M. Pan, R. Gianatassio, M. Schmidt, M. D. Eastgate and P. S. Baran, *J. Am. Chem. Soc.*, 2016, **138**, 2174.
- 37 D. Haas, J. M. Hammann, R. Greiner and P. Knochel, *ACS Catal.*, 2016, **6**, 1540.
- 38 H. Xu, J. B. Diccianni, J. Katigbak, C. Hu, Y. Zhang and T. Diao, *J. Am. Chem. Soc.*, 2016, **138**, 4779.
- 39 S. Yu, Y. Dudkina, H. Wang, K. V. Kholin, M. K. Kadirov, Y. H. Budnikova and D. A. Vicic, *Dalton Trans.*, 2015, **44**, 19443.
- 40 N. M. Camasso and M. S. Sanford, *Science*, 2015, **347**, 1218.
- 41 B. Mougang-Soume, F. Belanger-Gariepy and D. Zargarian, *Organometallics*, 2014, **33**, 5990.
- 42 J. P. Cloutier, B. Vabre, B. Mougang-Soume and D. Zargarian, *Organometallics*, 2015, **34**, 133.
- 43 W. Zhou, J. W. Schultz, N. P. Rath and L. M. Mirica, *J. Am. Chem. Soc.*, 2015, **137**, 7604.
- 44 J. R. Bour, N. M. Camasso and M. S. Sanford, *J. Am. Chem. Soc.*, 2015, **137**, 8034.
- 45 D. M. Grove, G. Van Koten, P. Mul, A. A. H. Van der Zeijden, J. Terheijden, M. C. Zoutberg and C. H. Stam, *Organometallics*, 1986, **5**, 322.
- 46 L. A. van de Kuil, Y. S. J. Veldhuizen, D. M. Grove, J. W. Zwikker, L. W. Jenneskens, W. Drenth, W. J. J. Smeets, A. L. Spek and G. van Koten, *J. Organomet. Chem.*, 1995, **488**, 191.
- 47 D. M. Grove, G. van Koten, R. Zoet, N. W. Murrall and A. J. Welch, *J. Am. Chem. Soc.*, 1983, **105**, 1379.
- 48 D. M. Grove, G. van Koten, P. Mul, R. Zoet, J. G. M. van der Linden, J. Legters, J. E. J. Schmitz, N. W. Murrall and A. J. Welch, *Inorg. Chem.*, 1988, **27**, 2466.
- 49 V. M. Iluc, A. J. M. Miller, J. S. Anderson, M. J. Monreal, M. P. Mehn and G. L. Hillhouse, *J. Am. Chem. Soc.*, 2011, **133**, 13055.
- 50 F. Z. Tang, N. P. Rath and L. M. Mirica, *Chem. Commun.*, 2015, **51**, 3113.
- 51 B. Zheng, F. Tang, J. Luo, J. W. Schultz, N. P. Rath and L. M. Mirica, *J. Am. Chem. Soc.*, 2014, **136**, 6499.
- 52 W. Zhou, S. Zheng, J. W. Schultz, N. P. Rath and L. M. Mirica, *J. Am. Chem. Soc.*, 2016, **138**, 5777.
- 53 W. Zhou, N. P. Rath and L. M. Mirica, *Dalton Trans.*, 2016, **45**, 8693.
- 54 G. J. M. Gruter, O. S. Akkerman and F. Bickelhaupt, *J. Org. Chem.*, 1994, **59**, 4473.
- 55 J. R. Khusnutdinova, N. P. Rath and L. M. Mirica, *J. Am. Chem. Soc.*, 2010, **132**, 7303.
- 56 E. Lee, J. M. Hooker and T. Ritter, *J. Am. Chem. Soc.*, 2012, **134**, 17456.
- 57 G. van Koten and D. Milstein, *Organometallic Pincer Chemistry*, Springer, Berlin, Heidelberg, 2013.
- 58 D. Zargarian, A. Castonguay and D. M. Spasyuk, *Top. Organomet. Chem.*, 2013, **40**, 131.
- 59 X. Lefevre, D. M. Spasyuk and D. Zargarian, *J. Organomet. Chem.*, 2011, **696**, 864.
- 60 S. M. Tetrick and R. A. Walton, *Inorg. Chem.*, 1985, **24**, 3363.
- 61 J. P. Farr, M. J. Abrams, C. E. Costello, A. Davison, S. J. Lippard and A. G. Jones, *Organometallics*, 1985, **4**, 139.
- 62 W. D. Jones and W. P. Kosar, *Organometallics*, 1986, **5**, 1823.